



Contents lists available at ScienceDirect

# Bioorganic & Medicinal Chemistry Letters

journal homepage: [www.elsevier.com/locate/bmcl](http://www.elsevier.com/locate/bmcl)

## Tanzawaic acid derivatives from a marine isolate of *Penicillium* sp. (SF-6013) with anti-inflammatory and PTP1B inhibitory activities



Tran Hong Quang<sup>a,b</sup>, Nguyen Thi Thanh Ngan<sup>a,b</sup>, Wonmin Ko<sup>a,c</sup>, Dong-Cheol Kim<sup>a,c</sup>, Chi-Su Yoon<sup>a,c</sup>, Jae Hak Sohn<sup>d</sup>, Jung Han Yim<sup>e</sup>, Youn-Chul Kim<sup>a,c,\*</sup>, Hyuncheol Oh<sup>a,c,\*</sup>

<sup>a</sup> College of Pharmacy, Wonkwang University, Iksan 570-749, Republic of Korea

<sup>b</sup> Institute of Marine Biochemistry, Vietnam Academy of Science and Technology (VAST), 18 Hoang Quoc Viet, Cau Giay, Hanoi, Viet Nam

<sup>c</sup> Hanbang Body-Fluid Research Center, Wonkwang University, Iksan 570-749, Republic of Korea

<sup>d</sup> College of Medical and Life Sciences, Silla University, Busan 617-736, Republic of Korea

<sup>e</sup> Korea Polar Research Institute, KORDI, 7-50 Songdo-dong, Yeosu-gu, Incheon 406-840, Republic of Korea

### ARTICLE INFO

#### Article history:

Received 6 August 2014

Revised 17 September 2014

Accepted 9 October 2014

Available online 17 October 2014

#### Keywords:

Marine-derived fungus

*Penicillium*

Anti-inflammatory

PTP1B

### ABSTRACT

Chemical investigation of a marine-derived fungus *Penicillium* sp. SF-6013 resulted in the discovery of a new tanzawaic acid derivative, 2*E*,4*Z*-tanzawaic acid D (**1**), together with four known analogues, tanzawaic acids A (**2**) and D (**3**), a salt form of tanzawaic acid E (**4**), and tanzawaic acid B (**5**). Their structures were mainly determined by analysis of NMR and MS data, along with chemical methods. Preliminary screening for anti-inflammatory effects in lipopolysaccharide (LPS)-activated microglial BV-2 cells showed that compounds **1**, **2**, and **5** inhibited the production of nitric oxide (NO) with IC<sub>50</sub> values of 37.8, 7.1, and 42.5 μM, respectively. Compound **2** also inhibited NO production in LPS-stimulated RAW264.7 murine macrophages with an IC<sub>50</sub> value of 27.0 μM. Moreover, these inhibitory effects correlated with the suppressive effect of compound **2** on inducible nitric oxide synthase (iNOS) and cyclooxygenase-2 (COX-2) expression in LPS-stimulated RAW264.7 and BV2 cells. In addition, compounds **2** and **5** significantly inhibited the activity of protein tyrosine phosphatase 1B (PTP1B) with the same IC<sub>50</sub> value (8.2 μM).

© 2014 Elsevier Ltd. All rights reserved.

The fungal genus *Penicillium* comprises more than 300 species,<sup>1</sup> which are known to produce secondary metabolites with chemical structures of various classes, including ergot alkaloids, diketopiperazines, benzodiazepines, quinolines, quinazolines, and polyketides.<sup>2</sup> In the course of our continuing search for bioactive secondary metabolites from marine-derived fungi,<sup>3,4</sup> we investigated the chemistry of an extract obtained from the cultures of a marine-derived isolate of the *Penicillium* sp. (SF-6013). Herein we describe the isolation and structural elucidation of the secondary metabolites (**1–5**) encountered in this investigation. Furthermore, the biological effects of the metabolites are also reported.

The *Penicillium* sp. SF-6013 was isolated from the sea urchin *Brisaster latifrons* collected from the Sea of Okhotsk (N 53°22.626' E 144°24.200') on January 28, 2009. The sample (1 g) was ground using a mortar and pestle and mixed with sterile seawater (10 mL). A portion (0.1 mL) of the sample was processed using the spread plate method in potato dextrose agar (PDA) medium containing seawater. The plate was incubated at 25 °C for 14 days. After subculturing the isolates several times, the final pure cultures

were selected and preserved at –70 °C. Strain SF-6013 was identified based on analysis of the ribosomal RNA (rRNA) sequences. A GenBank search using the 28S rRNA gene of SF-6013 (GenBank accession number KF745793) indicated *Penicillium steckii* (HM469415), *Penicillium chrysogenum* (FJ890400), and *Penicillium paxilli* (FJ890408), as the closest matches showing sequence identities of 99.63%, 98.64%, and 98.02%, respectively. Therefore, the marine-derived fungal strain SF-6013 was characterized as part of the *Penicillium* sp., but was not definitively identified to species.

The fungal strain was cultured on petri plates of PDA in media containing 3% NaCl at 25 °C for a period of 10 days. The cultured media was extracted with EtOAc, and the resultant extract was concentrated in vacuo to provide a residue. The residue was subjected to multiple chromatographic steps, including reversed-phase C<sub>18</sub>, silica gel preparative TLC, and semi-preparative HPLC to give metabolites **1–5** (Fig. 1).<sup>5</sup>

The three known metabolites were identified as tanzawaic acids A (**2**), D (**3**), and B (**5**) by comparative analyses of their NMR, MS, and optical rotation data with those of reported compounds.<sup>6</sup>

Compound **1** was isolated as a colorless and viscous oil.<sup>7</sup> The molecular formula of **1** was established as C<sub>18</sub>H<sub>22</sub>O<sub>3</sub> by the observation of a pseudomolecular ion peak at *m/z* 285.1481 [M–H]<sup>–</sup> in the

\* Corresponding authors. Tel.: +82 63 850 6815; fax: +82 63 852 8836.

E-mail addresses: [yckim@wonkwang.ac.kr](mailto:yckim@wonkwang.ac.kr) (Y.-C. Kim), [hoh@wku.ac.kr](mailto:hoh@wku.ac.kr) (H. Oh).

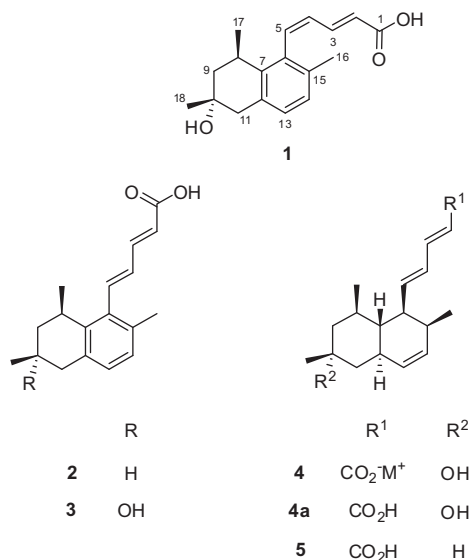


Figure 1. Structure of compounds 1–5.

HRESIMS and analysis of NMR data. The <sup>1</sup>H NMR spectrum (298 K, CD<sub>3</sub>OD) contained signals for two aliphatic double bonds [ $\delta_{\text{H}}$  6.00 (d,  $J = 15.2$  Hz, H-2), 6.80 (br, H-3), 6.40 (br, H-4), 6.71 (d,  $J = 11.2$  Hz, H-5)], two aromatic protons at  $\delta_{\text{H}}$  6.89 (d,  $J = 7.6$  Hz, H-13) and 6.95 (d,  $J = 7.6$  Hz, H-14), three methyl groups [ $\delta_{\text{H}}$  2.13 (s, H<sub>3</sub>-16), 1.11 (br, H<sub>3</sub>-17), 1.33 (s, H<sub>3</sub>-18)], and signals for aliphatic protons [ $\delta_{\text{H}}$  3.15 (br, H-8), 2.07 (m, H-9a), 1.61 (dd,  $J = 5.2, 14.4$  Hz, H-9b), 2.84 (d,  $J = 15.6$  Hz, H-11a), and 2.67 (d,  $J = 15.6$  Hz, H-11b)] (Table 1). Since the <sup>1</sup>H NMR spectrum of **1** acquired at 298 K in CD<sub>3</sub>OD was not suitable for structure determination owing to the presence of poorly resolved signals, attempts to obtain a better-resolved spectrum were made. Eventually, it was found that the <sup>1</sup>H NMR spectrum obtained at 253 K displayed signals split into pairs of sharp and well-resolved resonances (Table 1 and Fig. 2) with a population ratio of 1.0:0.8. In addition, the <sup>13</sup>C NMR and DEPT

spectra (253 K) of **1** displayed 36 carbon signals, including two sets of a carbonyl carbon, ten sp<sup>2</sup> carbons, four sp<sup>3</sup> carbons (two methylenes, one methine, and one oxygenated quaternary carbon), and three methyl groups (Table 1). These observations suggest that **1** has a medium conformational exchange rate on the NMR time scale at 298 K, while the conformational equilibrium is shifted to a slow exchange regime at a low temperature (253 K). This idea was also confirmed by the observation that the broad bumps in the <sup>1</sup>H NMR spectrum taken at 293 K in DMSO-*d*<sub>6</sub> (Supporting information, Fig. S4) turned into sharp signals at a higher temperature (328 K, DMSO-*d*<sub>6</sub>, Supporting information, Fig. S5), suggesting that the molecule is in a fast exchange regime. Therefore, the structure elucidation of **1** was conducted using analysis of 1D and 2D NMR data obtained at 253 K in CD<sub>3</sub>OD. The NMR data for two conformers were considered separately, and almost identical COSY and HMBC correlations for the respective protons and carbons in both conformers were observed (Fig. 3). The presence of a 1,2,3,4-tetrasubstituted benzene moiety was evident from signals for a pair of mutually *ortho*-coupled ( $J = 7.8$  Hz) aromatic protons, and observation of HMBC correlations from these protons to aromatic carbons. The aryl methyl C-16 was located at C-15 based on HMBC correlations from H-16 to C-6, C-14, and C-15, as well as from H-14 to C-16. The <sup>1</sup>H NMR spectrum showed the presence of two sets of two double bonds [conformer A (major):  $\delta_{\text{H}}$  5.95 (d, 15.6 Hz, H-2), 6.76 (dd,  $J = 10.8, 15.6$  Hz, H-3), 6.37 (t,  $J = 10.8$  Hz, H-4), and 6.71 (d, 10.8 Hz, H-5); conformer B (minor):  $\delta_{\text{H}}$  5.99 (d, 15.6 Hz, H-2), 6.86 (dd,  $J = 10.8$  Hz, 15.6, H-3), 6.47 (t,  $J = 10.8$  Hz, H-4), and 6.71 (d,  $J = 10.8$  Hz, H-5)] (Table 1). The  $J$  values for double bonds between C2–C3 and C4–C5 were 15.6 Hz and 10.8 Hz, respectively, in both conformers. Therefore, the respective configurations of double bonds in both conformers were assigned as *2E* and *4Z*. The presence of two sets of a penta-2,4-dienoic acid side chain (C1–C5) at C6 of the benzene ring was supported by COSY correlations between H-2/H-3, H-3/H-4, and H-4/H-5 as well as HMBC correlations from H-2 and H-3 to C-1 and from H-5 to C-6, C-7, and C-15 (Fig. 3). The presence of two sets of a CH<sub>3</sub>(17)–CH(8)–CH<sub>2</sub>(9) fragment was revealed by COSY correlations between H<sub>3</sub>-17/H-8, and between H-8/H<sub>2</sub>-9. This fragment was further extended to a C17–C8–C9–C10(C18)–C11 unit on the basis of HMBC correlations from H<sub>3</sub>-18

Table 1  
<sup>1</sup>H and <sup>13</sup>C NMR data for **1** at fast (298 K) and slow exchange (253 K)

Position	<b>1</b> (298 K) $\delta_{\text{H}}^{\text{a,b}}$ ( $J$ in Hz)	Conformer A (253 K)		Conformer B (253 K)	
		$\delta_{\text{C}}^{\text{a,c}}$	$\delta_{\text{H}}^{\text{a,d}}$ ( $J$ in Hz)	$\delta_{\text{C}}^{\text{a,c}}$	$\delta_{\text{H}}^{\text{a,d}}$ ( $J$ in Hz)
1		175.4		175.4	
2	6.00 (d, 15.2)	130.9	5.95 (d, 15.6)	130.9	5.99 (d, 15.6)
3	6.80 (br)	137.5	6.76 (dd, 10.8, 15.6)	138.4	6.86 (dd, 10.8, 15.6)
4	6.40 (br)	129.9	6.37 (t, 10.8)	131.8	6.47 (t, 10.8)
5	6.71 (d, 11.2)	136.4	6.71 (d, 10.8)	136.1	6.71 (d, 10.8)
6		136.2		135.9	
7		140.2		141.3	
8	3.15 (br)	30.5	3.15 (dd, 6.6, 13.8)	31.1	3.08 (dd, 6.6, 13.8)
9	2.07 (m)	46.0	2.06 (m)	46.0	2.06 (m)
	1.61 (dd, 5.2, 14.4)		1.56 (dd, 5.4, 13.8)		1.59 (dd, 4.8, 13.8)
10		69.9		70.7	
11	2.84 (d, 15.6)	44.8	2.83 (d, 15.0)	44.4	2.82 (d, 15.6)
	2.67 (br d, 15.6)		2.69 (br d, 14.4)		2.64 (dd, 1.8, 15.6)
12		133.6		133.6	
13	6.89 (d, 7.6)	129.8	6.89 (d, 7.8)	129.8	6.89 (d, 7.8)
14	6.95 (d, 7.6)	128.1	6.95 (d, 7.8)	128.7	6.97 (d, 7.8)
15		135.1		135.0	
16	2.13 (s)	20.8	2.11 (s)	21.1	2.13 (s)
17	1.11 (br)	22.7	1.14 (d, 7.2)	23.7	1.07 (d, 6.6)
18	1.33 (s)	30.8	1.29 (s)	31.2	1.33 (s)

<sup>a</sup> Recorded in CD<sub>3</sub>OD.

<sup>b</sup> Recorded in 400 MHz.

<sup>c</sup> Recorded in 150 MHz.

<sup>d</sup> Recorded in 600 MHz.

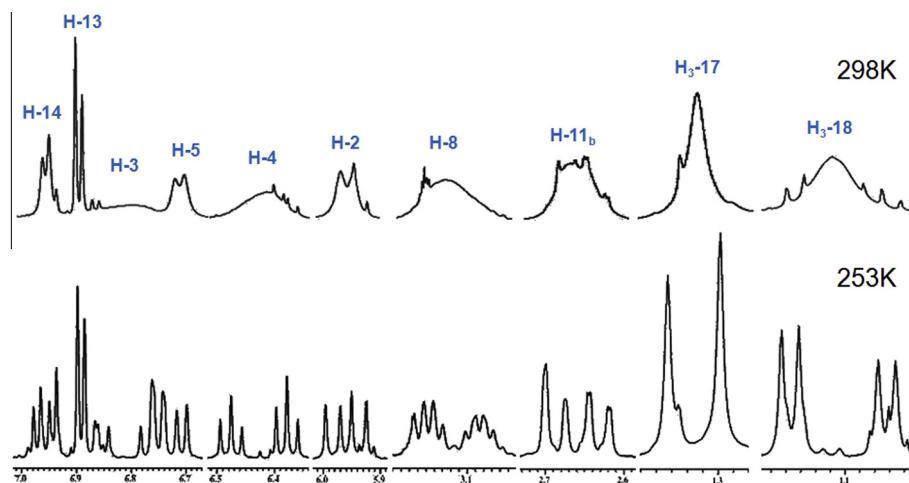


Figure 2. Regional expansions of the  $^1\text{H}$  NMR spectra of **1** in  $\text{CD}_3\text{OD}$  acquired at 253 and 298 K.

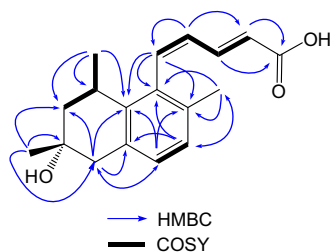


Figure 3. Selected HMBC and COSY correlations of **1**.

to C-9, C-10, and C-11. HMBC correlations from H<sub>2</sub>-11 to C-7, C-12, and C-13, from H<sub>3</sub>-17 to C-7, and from H-13 to C-7 and C-11 indicated the connections of C7C8 and C11C12, providing tetrahydronaphthalene moiety in **1**. From these analyses, in conjunction with comparison of the NMR data for **1** with those of the related metabolite, tanzawaic acid D<sup>6</sup>, the planar structure of **1** was

established as shown. The relative configuration of **1** was determined by analysis of the NOESY spectrum and comparison with the reported configurations of related metabolites.<sup>6,8</sup> NOESY correlations between H<sub>3</sub>-17/H-11a, H<sub>3</sub>-17/H-9b, H-11a/H<sub>3</sub>-18, and H<sub>3</sub>-18/H-9b suggested that H<sub>3</sub>-17 and H<sub>3</sub>-18 are located on the same face of the molecule. Finally, the structure of **1** was established as 2*E*,4*Z*-tanzawaic acid D. It is noteworthy that compound **1** is a sole tanzawaic acid type metabolite possessing *Z* configuration at the C-4 position, and this difference from the other tanzawaic acid derivatives may contribute to the aforementioned conformational behavior, which is unprecedented among these metabolites. Supporting this hypothesis, the  $^1\text{H}$  NMR spectrum (acquired at 295 K) of tanzawaic acid D (**3**), of which the structure is almost identical to that of **1** except for the presence of a 4*E* configuration at C-4, displayed well resolved  $^1\text{H}$  NMR signals (Figs. S13 and S14, Supporting information). This observation indicated that the presence of a 4*Z* configuration in **1** is the cause of a medium range of conformational exchange between conformers of **1** at room temperature. Furthermore, when carbon chemical shift differences between

Table 2  
 $^1\text{H}$  and  $^{13}\text{C}$  NMR data for **4** and **4a**

Position	<b>4</b>		<b>4a</b>	
	$\delta_{\text{C}}^{\text{a,b}}$	$\delta_{\text{H}}^{\text{a,c}}$ (J in Hz)	$\delta_{\text{C}}^{\text{a,b}}$	$\delta_{\text{H}}^{\text{a,c}}$ (J in Hz)
1	170.6		167.6	
2	132.0	5.67 (d, 15.2)	119.8	5.79 (d, 15.2)
3	135.7	6.67 (dd, 10.8, 15.2)	144.6	7.20 (10.8, 15.2)
4	127.7	6.01 (dd, 10.8, 15.2)	126.2	6.20 (dd, 10.8, 15.2)
5	141.9	5.86 (dd, 10.4, 15.2)	149.8	6.32 (dd, 10.4, 15.2)
6	48.3	2.33 (ddd, 5.0, 10.0, 10.4)	48.3	2.40 (ddd, 5.6, 10.0, 10.0)
7	45.7	0.84 (m)	45.7	0.86 (m)
8	31.6	1.61 (m)	31.6	1.63 (m)
9	49.9	1.47 (m)	49.8	1.53 (m)
		1.04 (m)		1.03 (m)
10	67.7		67.7	
11	45.1	1.52 (m)	45.0	1.57 (m)
		1.06 (m)		1.10 (m)
12	36.8	2.21 (m)	37.0	2.22 (m)
13	131.8	5.35 (d, 9.6)	131.8	5.37 (d, 9.6)
14	132.2	5.56 (m)	131.9	5.56 (m)
15	37.3	2.09 (m)	36.6	2.12 (m)
16	16.2	0.90 (d, 6.8)	16.2	0.91 (d, 6.8)
17	22.3	0.86 (d, 6.4)	22.2	0.83 (d, 6.4)
18	31.2	1.07 (s)	31.2	1.07 (s)

<sup>a</sup> Recorded in  $\text{DMSO}-d_6$ .

<sup>b</sup> Recorded in 100 MHz.

<sup>c</sup> Recorded in 400 MHz.

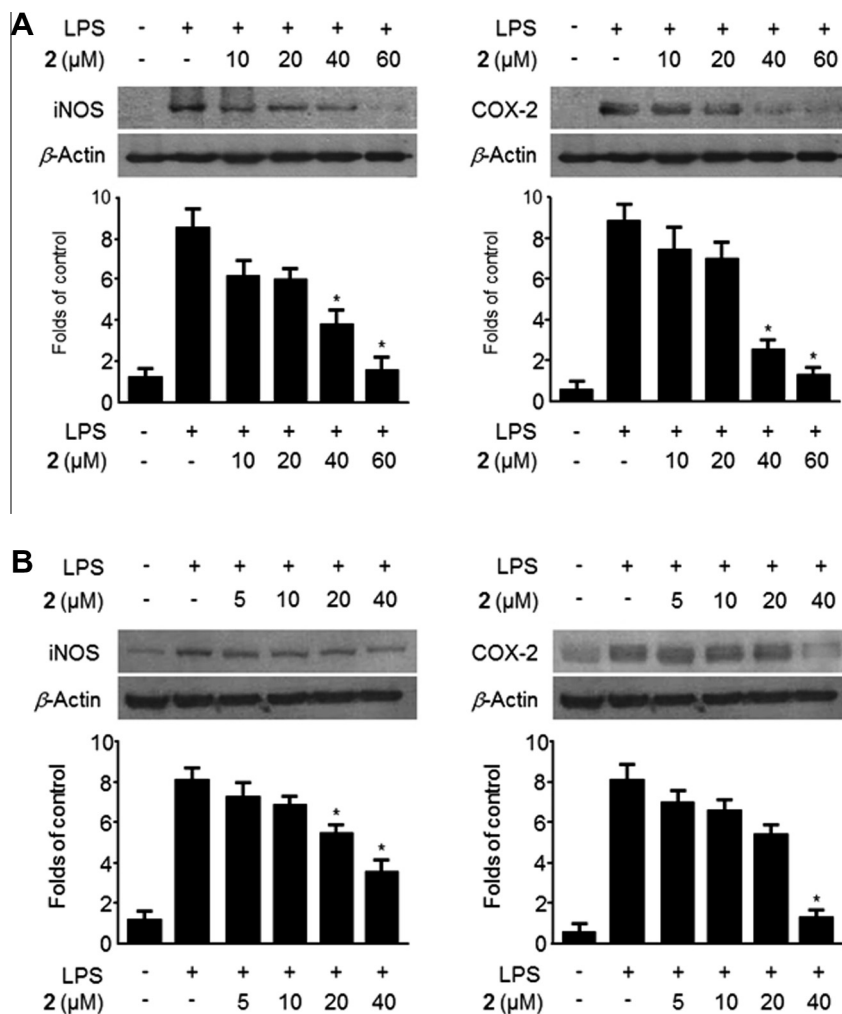


**Figure 4.** Effects of **2** on lipopolysaccharide (LPS)-induced inducible nitric oxide synthase (iNOS) and cyclooxygenase-2 (COX-2) protein expression in RAW264.7 (A) and BV2 cells (B). RAW264.7 and BV2 cell microglia were pretreated for 1 h with the indicated concentrations of **2**, and then treated for 18 h with LPS (0.5 μg/mL). Western blot analyses for iNOS and COX-2 expression were performed and representative blots of three independent experiments are shown.

two conformers were mapped (Fig. S10, Supporting information), significant chemical shift differences were observed at the C-3 ( $\Delta\delta_C = +0.9$ ), C-4 ( $\Delta\delta_C = +1.9$ ), C-7 ( $\Delta\delta_C = +1.1$ ), and C-17 ( $\Delta\delta_C = +1.0$ ) positions. These data suggest that the conformational behavior of **1** may be the result of a hindered rotation of the penta-2*E*,4*Z*-dienoic acid side chain by the methyl group at C-8. However, the differentiation of two possible conformers of **1** may require further study of the molecular dynamics simulation and kinetics of the interconversion.<sup>9–11</sup>

Compound **4** was isolated as a colorless gum.<sup>7</sup> The <sup>1</sup>H NMR of **4** showed signals for six olefinic protons at  $\delta_H$  5.67 (d,  $J = 15.2$  Hz, H-2), 6.67 (dd,  $J = 10.8, 15.2$  Hz, H-3), 6.01 (dd,  $J = 10.8, 15.2$  Hz, H-4), 5.86 (dd,  $J = 10.4, 15.2$  Hz, H-5), 5.35 (d,  $J = 9.6$  Hz, H-13), and 5.56 (m, H-14), and three methyl groups at  $\delta_H$  0.90 (d,  $J = 6.8$  Hz, H<sub>3</sub>-16), 0.86 (d,  $J = 6.4$  Hz, H<sub>3</sub>-17), and 1.07 (s, H<sub>3</sub>-18) (Table 2). The <sup>13</sup>C NMR and DEPT spectra showed 18 signals, including one carbonyl carbon, six sp<sup>2</sup> carbons, eight sp<sup>3</sup> carbons (including two methylenes, five methines, and one oxygenated quaternary carbon), and three methyl groups. Analysis of the <sup>1</sup>H and <sup>13</sup>C NMR spectra indicated the presence of a penta-2,4-dienoic acid side chain in the structure of **4**. The large coupling constants (15.2 Hz) between H-2/H-3 and H-4/H-5 indicated *trans*-configuration for the  $\Delta^{2,3}$  and  $\Delta^{4,5}$  double bonds. The penta-2*E*,4*E*-dienoic acid was located at C-6 based on the COSY correlation between

H-5 and H-6. The position of substructure C6C15 was determined by detailed analysis of HMQC, COSY, and HMBC correlations (data not shown). Comparison of the <sup>1</sup>H and <sup>13</sup>C NMR data of **4** with those of tanzawaic acid E,<sup>12</sup> a free carboxylic acid previously isolated from *Penicillium steckii*, revealed that the structures of these compounds are similar, except for the shift differences at the side chain. Although the configurations of two olefins at C-2 and C-4 of both compounds are *trans*, the <sup>1</sup>H and <sup>13</sup>C NMR data of the side chains of each were very different [**4**:  $\delta_C$  170.6 (C-1),  $\delta_H$  5.67/ $\delta_C$  132.0 (C-2),  $\delta_H$  6.67/ $\delta_C$  135.7 (C-3),  $\delta_H$  6.01/ $\delta_C$  127.7 (C-4), and  $\delta_H$  5.86/ $\delta_C$  141.9 (C-5) versus tanzawaic acid E:  $\delta_C$  167.8 (C-1),  $\delta_H$  5.80/ $\delta_C$  119.9 (C-2),  $\delta_H$  7.22/ $\delta_C$  144.8 (C-3),  $\delta_H$  6.22/ $\delta_C$  126.4 (C-4), and  $\delta_H$  6.34/ $\delta_C$  150.0 (C-5)],<sup>12</sup> suggesting that **4** was obtained as a carboxylate salt (Table 2). Although ESIMS data of **4** could not provide the identity of a counter cation, the presence of a carboxylate ion was confirmed by the conversion of **4** to a free carboxylic acid form (**4a**) with treatment of 0.1 N HCl.<sup>13</sup> The <sup>1</sup>H and <sup>13</sup>C NMR data of **4a** were exactly matched with those reported for tanzawaic acid E.<sup>12</sup> Based on their similar specific optical rotation values [**4**:  $[\alpha]_D^{23} +74.2^\circ$  ( $c = 0.12$ , MeOH); **4a**:  $[\alpha]_D^{23} +51.8^\circ$  ( $c = 0.06$ , MeOH); tanzawaic acid E:  $[\alpha]_D^{20} +45.5^\circ$  ( $c = 0.11$ , MeOH)], it was suggested that **4** and tanzawaic acid E share the same absolute configuration.<sup>12</sup> Thus, the structure of **4** was established as a salt form of tanzawaic acid E.

Inflammation is a normal immune process to protect the body from infection or tissue injury. During the inflammatory process, the stimulated immune monocytes and macrophages overexpress inducible nitric oxide synthase (iNOS) and cyclooxygenase-2 (COX-2) and secrete increased amounts of inflammatory mediators such as nitric oxide (NO), prostaglandin E<sub>2</sub> (PGE<sub>2</sub>), and interleukin-1 $\beta$  (IL-1  $\beta$ ). Overproduction of these factors is involved in cell damage and inflammatory diseases, such as rheumatoid arthritis, diabetes, and chronic hepatitis.<sup>14–17</sup> Therefore, inhibitors of these inflammatory mediators would be an effective therapeutic approach for the prevention and treatment of inflammatory diseases. Lipopolysaccharide (LPS)-induced RAW264.7 murine macrophages are generally used as a model system in the study of macrophage activation and the release of inflammatory mediators. Similarly, microglia BV2 cells, an immortalized murine microglia cell line, are used as an in vitro model for neuroinflammatory responses. The inhibitory effects of the isolated compounds on NO production were evaluated in LPS-stimulated RAW264.7 and BV2 cells (Supporting information). Among the isolated compounds, only **2** showed a moderate inhibitory effect in RAW264.7 cells, with an IC<sub>50</sub> value of 27.0  $\mu$ M, whereas **1**, **2**, and **5** inhibited NO production in BV2 cells, with IC<sub>50</sub> values of 37.8, 7.1, and 42.5  $\mu$ M, respectively. Based on these observations, compound **2** was further evaluated for its inhibitory effects on iNOS and COX-2 expression in LPS-stimulated RAW264.7 and BV2 cells using western blot analysis (Supporting information). As shown in Figure 4, compound **2** inhibited the expression of iNOS and COX-2 in a dose-dependent manner in both LPS-stimulated RAW264.7 and BV2 cells, while the expression of the house-keeping protein,  $\beta$ -actin, was unchanged by the presence of **2** at the same concentrations. Furthermore, compound **2** exhibited significant inhibitory effects on PGE<sub>2</sub> production, with IC<sub>50</sub> values of 17.5 and 15.7  $\mu$ M in LPS-stimulated RAW264.7 and BV2 cells, respectively. However, compound **2** only inhibited IL-1 $\beta$  production in LPS-stimulated BV2 cells, with an IC<sub>50</sub> value of 21.9  $\mu$ M. These results provide a rationale for further studies of compound **2** for the development of an anti-inflammatory agent.

Protein tyrosine phosphatase 1B (PTP1B) is the major negative regulator of the insulin and leptin signaling cascades. Current studies have demonstrated PTP1B as a promising drug discovery target for the treatment of insulin resistance, diabetes, and obesity.<sup>18</sup> In the evaluation of the inhibitory effects of the compounds against PTP1B activity (Supporting information), compounds **2** and **5** showed equivalent inhibitory effects against PTP1B activity with IC<sub>50</sub> values of 8.2  $\mu$ M. On the other hand, compounds **1** and **3** showed only 27.3% and 24.1% inhibitory effects, respectively, at a 30  $\mu$ M level, while compound **4a** was inactive at this level. Based on the different inhibitory effects against PTP1B among the similar structures, it could be suggested that the presence of the hydroxyl group at C-10 might be a key structural feature in diminishing the PTP1B inhibitory effects of tanzawaic acid derivatives. Since tanzawaic acids A–D were first isolated in 1997 from *Penicillium citrinum*,<sup>6</sup> twelve derivatives have been identified from different *Penicillium* species.<sup>6,8,12,19</sup> Among these tanzawaic acids, the presence of a hydroxy group at C-10 was found in the structures of tanzawaic acids D, E, G, and L, whereas the other tanzawaic acids contain other functional groups such as carboxylic acid, oxymethylene, and methyl groups at the C-10 or C-14 positions (Fig. S23, Supporting information). Therefore, further PTP1B inhibitory assays on the remaining tanzawaic acids might provide clearer insight into the structure-activity relationships of these metabolites. In addition to this, further studies of these metabolites with respect to the mode of inhibition against PTP1B, as well as their

anti-diabetic effects in cellular and animal models, may lead to the identification of a new class of PTP1B inhibitors.

## Acknowledgment

This research was supported by a Grant from the Ministry of Oceans and Fisheries' R&D project (PM13030).

## Supplementary data

Supplementary data associated with this article can be found, in the online version, at <http://dx.doi.org/10.1016/j.bmcl.2014.10.035>.

## References and notes

- Kirk, P. M.; Cannon, P. F.; Minter, D.; Stalpers, J. A. *Dictionary of the Fungi*, 10th ed.; CABI: Europe-UK, 2008.
- Kozlovskii, A. G.; Zhelifonova, V. P.; Antipova, T. V. *Appl. Biochem. Microbiol.* **2013**, *49*, 1.
- Quang, T. H.; Lee, D.-S.; Sohn, J. H.; Kim, Y.-C.; Oh, H. *Bull. Korean Chem. Soc.* **2013**, *34*, 3109.
- Lee, D. S.; Ko, W.; Quang, T. H.; Kim, K. S.; Sohn, J. H.; Jang, J. H.; Ahn, J. S.; Kim, Y. C.; Oh, H. *Mar. Drugs* **2013**, *11*, 4510.
- The fungal strain was cultured on 100 petri plates (90-mm), each containing 20 mL of PDA with 3% NaCl. Plates were individually inoculated with 2 mL seed cultures of the fungal strain and incubated at 25 °C for a period of 10 days. Extraction of the combined agar media with methylethylketone (2 L) provided an organic phase, which was then concentrated in vacuo to yield an extract residue (510 mg). The dried extract was subjected to C<sub>18</sub> flash column chromatography (5  $\times$  26 cm), eluting with a stepwise gradient of 20, 40, 60, 80, and 100% (v/v) MeOH in H<sub>2</sub>O (500 mL each) to give fractions 6013-1-6, respectively. Fraction 6013-4 (49 mg) was subjected to RP C<sub>18</sub> HPLC, eluted with MeOH in H<sub>2</sub>O (20–100% v/v) in 50 min to yield eight subfractions, 6013-4-1-8. Subfraction 6013-4-5 (6.0 mg) was separated by preparative TLC, using *n*-hexane-EtOAc (1:6) as eluents to give **1** (2.0 mg) and **3** (1.0 mg). From subfraction 6013-4-6 (3.3 mg), **4** (1.0 mg) was isolated using preparative TLC, eluted with *n*-hexane/acetone 2:3. Fraction 6013-5 (110 mg) was chromatographed over Sephadex LH-20 column, eluting with CH<sub>2</sub>Cl<sub>2</sub>/MeOH 20:1 to give subfractions 6013-5-1-5. Subfraction 6013-5-4 (9.5 mg) was subjected to semi-preparative reversed-phase HPLC eluting with a gradient from 80% to 100% MeOH in H<sub>2</sub>O (0.1% formic acid) for 60 min to give **2** (1.5 mg, *t<sub>R</sub>* = 24.7 min) and **5** (2.0 mg, *t<sub>R</sub>* = 26.3 min).
- Kuramoto, M.; Yamada, K.; Shikano, M.; Yazawa, K.; Arimoto, H.; Okamura, T.; Uemura, D. *Chem. Lett.* **1997**, *26*, 885.
- 2*E,4Z*-Tanzawaic acid D (**1**): colorless and viscous oil; [ $\alpha$ ]<sub>D</sub><sup>23</sup> +100.8 (*c* = 0.25, MeOH); HR-ESIQTOFMS (negative mode): *m/z* 285.1481 [M–H]<sup>–</sup> (calcd. for C<sub>18</sub>H<sub>21</sub>O<sub>3</sub>, 285.1491); <sup>1</sup>H (CD<sub>3</sub>OD, 600 MHz) and <sup>13</sup>C NMR data (CD<sub>3</sub>OD, 150 MHz), see Table 1.
- Salt of tanzawaic acid E (**4**): colorless gum; [ $\alpha$ ]<sub>D</sub><sup>23</sup> +74.2 (*c* = 0.12, MeOH); HR-ESIQTOFMS (negative mode): *m/z* 289.1786 [M]<sup>–</sup> (calcd. for C<sub>18</sub>H<sub>25</sub>O<sub>3</sub>, 289.1804); <sup>1</sup>H (DMSO-*d*<sub>6</sub>, 400 MHz) and <sup>13</sup>C NMR data (DMSO-*d*<sub>6</sub>, 100 MHz), see Table 2.
- El-Neketi, M.; Ebrahim, W.; Lin, W.; Gedara, S.; Badria, F.; Saad, H. E.; Lai, D.; Proksch, P. *J. Nat. Prod.* **2013**, *76*, 1099.
- Costantino, V.; Fattorusso, E.; Mangoni, A.; Perinu, C.; Teta, R.; Panza, E.; Ianaro, A. *J. Org. Chem.* **2012**, *77*, 6377.
- Faraldos, J. A.; Wu, S.; Chappell, J.; Coates, R. M. *Tetrahedron* **2007**, *63*, 7733.
- Wong, H. F.; Brown, G. D. *Phytochemistry* **2002**, *59*, 529.
- Malmstrom, J.; Christophersen, C.; Frisvad, J. C. *Phytochemistry* **2000**, *54*, 301.
- Acidification of **4**: Compound **4** (1 mg) was dissolved in aqueous 0.1 N HCl (5 mL) and stirred for 30 min at 50 °C. The reaction mixture was then partitioned with EtOAc. The EtOAc layer was concentrated in vacuo to yield **4a** (0.7 mg). <sup>1</sup>H (DMSO-*d*<sub>6</sub>, 400 MHz) and <sup>13</sup>C NMR data (DMSO-*d*<sub>6</sub>, 100 MHz), see Table 2.
- Amin, A. R.; Attur, M.; Abramson, S. B. *Curr. Opin. Rheumatol.* **1999**, *11*, 202.
- Bombardieri, S.; Cattani, P.; Ciabattini, G.; Di Munno, O.; Pasero, G.; Patrono, C.; Pinca, E.; Pugliese, F. *Br. J. Pharmacol.* **1981**, *73*, 893.
- Pavlovic, D.; Chen, M. C.; Bouwens, L.; Eizirik, D. L.; Pipeleers, D. *Diabetes* **1999**, *48*, 29.
- Cuzzocrea, S.; Zingarelli, B.; Villari, D.; Caputi, A. P.; Longo, G. *Life Sci.* **1998**, *63*(PL2), 5.
- Liu, G.; Trevillyan, J. M. *Curr. Opin. Invest. Drugs* **2002**, *3*, 1608.
- Sandjo, L. P.; Thines, E.; Opatz, T.; Schuffler, A. *Beilstein J. Org. Chem.* **2014**, *10*, 251.